# Ternary Rare-Earth Selenides with the $U_3ScS_6$ Structure Type: Synthesis, Characterization, and Some Magnetic Properties of $Ln_3TSe_6$ (Ln = Sm, Gd; T = In, Cr) and $Tb_3CrSe_6$

**Olivier Tougait and James A. Ibers***

Department of Chemistry, Northwestern University, 2145 Sheridan Road, Evanston, Illinois 60208-3113

*Received December 22, 1999*

The new compounds $Ln_3TSe_6$ (Ln = Sm, Gd; T = In, Cr) and $Tb_3CrSe_6$ have been synthesized by the solid-state reactions of the elements at 850 °C. A KBr flux was used to promote crystal growth. These isostructural compounds crystallize with the $U_3ScS_6$ structure type. The crystal structure is built from $LnSe_7$ pseudo-octahedra or $LnSe_8$ bicapped trigonal prisms and $TSe_6$ octahedra. Magnetic measurements show that $Sm_3TSe_6$ (T = In, Cr) and $Tb_3CrSe_6$ are paramagnetic down to 5 K whereas $Gd_3CrSe_6$ undergoes an antiferromagnetic transition at 10 K. Crystal data: orthorhombic, *Pnnm*, $Z = 4$, $T = -120$ °C, (compound, $a$ (Å), $b$ (Å), $c$ (Å))—$Sm_3InSe_6$, 14.177(3), 17.352(4), 4.0625(8); $Gd_3InSe_6$, 14.071(3), 17.286(4), 4.0202(8); $Sm_3CrSe_6$, 14.032(3), 16.782(3), 3.9841(8); $Gd_3CrSe_6$, 13.938(3), 16.780(3), 3.9559(8); $Tb_3CrSe_6$, 13.885(3), 16.672(3), 3.9215(8).

## Introduction

New compounds containing a combination of d and f elements are of interest in solid-state chemistry and materials science because of their physical properties. Examples include the spectroscopic and electronic properties of materials such as Nd:YIG,[1] the permanent magnetic properties of $SmCo_5$ and $Nd_2Fe_{14}B$ alloys,[2] and the heavy fermion conductors $CeRu_2Si_2$[3] and $HoNi_2B_2C$[4] with their coexistence of superconductivity and magnetism.

Among the solid-state 3d/4f chalcogenides, the number of ternary compounds decreases dramatically as we move from the sulfides to the tellurides. Ternary 4f sulfides are known for all 3d metals, a few selenides are reported, usually characterized by X-ray powder methods,[5] and tellurides are only known for Cu, namely, for $LnCu_xTe_2$ ($0.5 \le x \le 0.28$; Ln = La, Ce, Pr, Nd, Sm, Gd, Ho). [6−8] Included among the sulfides are the misfit compounds of general formula $(LnS)_n(TS_2)_m$ that consist of the stacking of alternating layers of LnS and $TS_2$ where $T$ = 3d metal. This class of materials has been widely studied.[9,10]

With the exception of misfit-layer compounds, crystal structures of reported ternary 3d/4f sulfides consist of edge-sharing of polyhedra centered by rare-earth and 3d-block metal cations.[5] The rare-earth metals usually have a trigonal prismatic geometry, whereas the transition metals are usually tetrahedrally or octahedrally coordinated. The resulting joined polyhedra lie perpendicular to the short axis of a flat unit cell.

The impetus for the present research is to synthesize and characterize new 3d/4f selenides and tellurides. In the present article, we describe the synthesis, structures, and magnetic properties of five new ternary rare-earth selenides of the $U_3ScS_6$ structure type[11] in which U has been substituted by Ln = Sm, Gd, or Tb and Sc has been substituted by T = In or Cr. Although In is not a d-block metal, it does, like Cr, have a stable +III oxidation state and a preference for a coordination number of 6.

## Experimental Section

**Syntheses.** Sm (Alfa, 40 mesh 99.9%), Gd (Alfa, 40 mesh 99.9%), Tb (Alfa, 40 mesh 99.9%), In (Alfa, 325 mesh, 99.99%), Cr (Alfa, 325 mesh, 99.99%), and KBr (Alfa 99%) were stored in an Ar-filled glovebox and were used as received. Crystalline powders of $Ln_3TSe_6$ (Ln = Sm, Gd; T = In, Cr) and $Tb_3CrSe_6$ were obtained from the reactions of stoichiometric amounts of the elements. For those reactions involving In, 1.0 mmol of Ln (Ln = Sm, Gd), 0.33 mmol of In, and 2.0 mmol of Se, and for those reactions involving Cr, 1.125 mmol of Ln (Ln = Sm, Gd, Tb), 0.375 mmol of Cr, and 2.25 mmol of Se were loaded into fused silica tubes with an additional amount of 150−200 mg of KBr. The tubes were flame-sealed under a vacuum of $10^{-4}$ Torr, heated to 850 °C over a 48 h period, maintained at 850 °C for 96 h, cooled to 600 °C at 2.5 °C/h, and then the furnace was turned off. The final products were washed with $CH_3OH/H_2O$ to eliminate the flux and were dried with acetone. Black lustrous needles with typical dimensions of 0.3 mm × 0.02 mm × 0.02 mm suitable for further characterization were extracted from the polycrystalline materials. With the exception of $Gd_3InSe_6$, the reactions are essentially quantitative. Semiquantitative wavelength-dispersive spectrometry (WDS) analyses were carried out on several single crystals from each preparation with the use of a 570 or 3500N Hitachi scanning electron microscope (SEM). The results of 3/1/6 for Ln/T/Se are in very good agreement with those determinated from the X-ray structure refinements. No traces of O, K, or Br were detected. The crystals are stable in air.

**Crystal Structure Analyses.** X-ray diffraction data were collected on a Bruker Smart 1000 CCD diffractometer at −120 °C with the use

(1) Helszan, J. *YIG Resonators and Filters*; John Wiley & Sons: New York, 1985.
(2) Herbst, J. F. *Rev. Mod. Phys.* **1991**, *63*, 819−898.
(3) Gupta, L. C.; MacLaughlin, D. E.; Tien, C.; Godart, C.; Edwards, M. A.; Parks, R. D. *Phys. Rev. B* **1983**, *28*, 3673−3676.
(4) Goldman, A. I.; Stassis, C.; Canfield, P. C.; Zaretsky, J.; Dervenagas, P.; Cho, B. K.; Johnston, D. C.; Sternlieb, B. *Phys. Rev. B* **1994**, *50*, 9668−9671.
(5) Flahaut, J. In *Handbook on the Physics and Chemistry of Rare Earths*; Gschneidner, K. A., Jr.; Eyring, L. R., Eds.; North-Holland: Amsterdam, New York, Oxford, 1979; Vol. 4, pp 1−88.
(6) Pardo, M.-P.; Dung, N. H. *C. R. Acad. Sci. Paris* **1987**, *12*, 637−639.
(7) Dung, N.-H.; Pardo, M.-P.; Boy, P. *Acta Crystallogr., Sect. C: Cryst. Struct. Commun.* **1983**, *39*, 668−670.
(8) Huang, F. Q.; Brazis, P.; Kannewurf, C. R.; Ibers, J. A. *J. Am. Chem. Soc.* **2000**, *122*, 80−86.
(9) Wiegers, G. A. *Prog. Solid State Chem.* **1996**, *24*, 1−139.
(10) Meerschaut, A. *Curr. Opin. Solid State Mater. Sci.* **1996**, *1*, 250−256.
(11) Rodier, N.; Tien, V. *Acta Crystallogr., Sect. B: Struct. Crystallogr. Cryst. Chem.* **1976**, *32*, 2705−2707.

10.1021/ic9914802 CCC: $19.00 
Published on Web 03/29/2000

**Table 1.** X-ray Crystallographic Details[a]

| | $Sm_3InSe_6$ | $Gd_3InSe_6$ | $Sm_3CrSe_6$ | $Gd_3CrSe_6$ | $Tb_3CrSe_6$ |
|---|---|---|---|---|---|
| fw | 1039.63 | 1060.33 | 976.81 | 997.51 | 1002.52 |
| $a$ (Å) | 14.177(3) | 14.071(3) | 14.032(3) | 13.938(3) | 13.885(3) |
| $b$ (Å) | 17.352(4) | 17.286(4) | 16.782(3) | 16.780(3) | 16.672(3) |
| $c$ (Å) | 4.0625(8) | 4.0202(8) | 3.9841(8) | 3.9559(8) | 3.9215(8) |
| $V$ (Å$^3$) | 999.4(3) | 977.9(3) | 938.2(3) | 925.2(3) | 907.8(3) |
| $d_{calcd}$ (g cm$^{-3}$) | 6.910 | 7.202 | 6.916 | 7.161 | 7.335 |
| $\mu$ (cm$^{-1}$) | 414.2 | 446.7 | 428.2 | 458.9 | 482.23 |
| $R(F)^b$ | 0.0299 | 0.0273 | 0.0342 | 0.0374 | 0.0397 |
| $R_w(F_o^2)^c$ | 0.0618 | 0.0533 | 0.0662 | 0.0601 | 0.0737 |

[a] All five compounds crystallize with four formula units in space group *Pnnm* of the orthorhombic system, as observed at −120 °C. [b] $R(F) = \sum||F_o| - |F_c||/\sum|F_c|$. [c] $R_w(F_o^2) = [\sum w(F_o^2 - F_c^2)^2/\sum wF_o^4]^{1/2}$ where $w = 1/[\sigma^2(F_o^2) + (0.04F_o^2)^2]$.

**Table 2.** Selected Interatomic Distances (Å) for $Ln_3InSe_6$ (Ln = Sm, Gd)

| | $Sm_3InSe_6$ | $Gd_3InSe_6$ |
|---|---|---|
| Ln(1)−Se(2) | 2.8860(11) | 2.8605(10) |
| Ln(1)−Se(1) × 2 | 2.9053(7) | 2.8809(7) |
| Ln(1)−Se(4) × 2 | 2.9822(8) | 2.9582(8) |
| Ln(1)−Se(3) | 3.0552(10) | 3.0318(10) |
| Ln(1)−Se(6) | 3.0559(11) | 3.0398(10) |
| Ln(2)−Se(2) × 2 | 2.9550(8) | 2.9267(7) |
| Ln(2)−Se(1) × 2 | 3.0058(8) | 2.9784(11) |
| Ln(2)−Se(6) | 3.0107(11) | 2.9833(8) |
| Ln(2)−Se(3) × 2 | 3.0462(8) | 3.0275(8) |
| Ln(2)−Se(5) | 3.0631(10) | 3.0417(10) |
| Ln(3)−Se(3) × 2 | 2.9447(8) | 2.9123(8) |
| Ln(3)−Se(5) × 2 | 3.0034(8) | 2.9739(8) |
| Ln(3)−Se(4) × 2 | 3.0986(8) | 3.0758(8) |
| Ln(3)−Se(1) | 3.1988(10) | 3.1728(10) |
| Ln(3)−Se(6) | 3.2491(11) | 3.2156(11) |
| In(1)−Se(4) × 2 | 2.7308(10) | 2.7250(9) |
| In(1)−Se(6) × 4 | 2.7336(7) | 2.7208(7) |
| In(2)−Se(2) × 2 | 2.5531(9) | 2.5528(9) |
| In(2)−Se(5) × 4 | 2.8513(7) | 2.8453(7) |

of monochromatized Mo Kα radiation ($\lambda = 0.710\ 73$ Å). The diffracted intensities generated by a scan of 0.3° in $\omega$ were recorded on 1271 frames covering more than a hemisphere of the Ewald sphere for $Ln_3InSe_6$ (Ln = Sm, Gd) and $Ln_3CrSe_6$ (Ln = Sm, Tb) and on 1878 frames for $Gd_3CrSe_6$. The exposure times were 30 s/frame for $Gd_3InSe_6$, 25 s/frame for $Gd_3CrSe_6$ and $Tb_3CrSe_6$, 20 s/frame for $Sm_3CrSe_6$, and 15 s/frame for $Sm_3InSe_6$. For each compound, cell refinement and data reduction were carried out with the use of the program SAINT[12] and a face-indexed absorption correction was made with the use of the program XPREP.[13] Then the program SADABS[12] was employed to make incident beam and decay corrections. All structures were solved with the direct methods program SHELXS of the SHELXTL-PC suite of programs[13] and refined by full-matrix least-squares techniques. Final refinements included anisotropic displacement parameters and a secondary extinction correction. Some crystallographic details are presented in Table 1. Others may be found in Supporting Information. Selected bonds distances for $Ln_3InSe_6$ (Ln = Sm, Gd) are given in Table 2 and those for $Ln_3CrSe_6$ (Ln = Sm, Gd, Tb) are given in Table 3.

**X-ray Powder Diffraction Measurements.** The purity of the samples was confirmed by a comparison of X-ray powder diffraction patterns (obtained on a Rigaku powder diffractometer equipped with monochromatized Cu $K\alpha_1$ radiation) with those calculated from the X-ray crystal structures.[14] All powder patterns, with the exception of that for $Gd_3InSe_6$, were fully indexable. The sample of $Gd_3InSe_6$ was contaminated with an unknown phase.

(12) *SMART Version 5.054 Data Collection* and *SAINT-Plus Version 6.0 Data Processing Software for the SMART System*; Bruker Analytical X-Ray Instruments, Inc.: Madison, WI, 1999.

(13) Sheldrick, G. M. *SHELXTL DOS/Windows/NT*, version 5.10; Bruker Analytical X-Ray Instruments, Inc.: Madison, WI, 1997.

**Table 3.** Selected Interatomic Distances (Å) for $Ln_3CrSe_6$ (Ln = Sm, Gd, Tb)

| | $Sm_3CrSe_6$ | $Gd_3CrSe_6$ | $Tb_3CrSe_6$ |
|---|---|---|---|
| Ln(1)−Se(2) | 2.8692(11) | 2.8469(13) | 2.8305(14) |
| Ln(1)−Se(1) × 2 | 2.8973(8) | 2.8738(9) | 2.8579(9) |
| Ln(1)−Se(4) × 2 | 2.9335(9) | 2.9144(10) | 2.8962(10) |
| Ln(1)−Se(6) | 2.9777(12) | 2.9638(13) | 2.9449(14) |
| Ln(1)−Se(3) | 3.0058(11) | 2.9930(13) | 2.9755(13) |
| Ln(2)−Se(2) × 2 | 2.9462(8) | 2.9221(9) | 2.9004(10) |
| Ln(2)−Se(1) × 2 | 2.9704(8) | 2.9496(9) | 2.9311(10) |
| Ln(2)−Se(3) × 2 | 3.0053(8) | 2.9883(9) | 2.9699(10) |
| Ln(2)−Se(5) | 3.0627(11) | 3.0499(13) | 3.0382(13) |
| Ln(2)−Se(6) | 3.0855(12) | 3.0523(13) | 3.0259(13) |
| Ln(3)−Se(3) × 2 | 2.9285(8) | 2.9073(9) | 2.8813(10) |
| Ln(3)−Se(4) × 2 | 3.0019(8) | 2.9911(9) | 2.9667(10) |
| Ln(3)−Se(5) × 2 | 3.0311(9) | 3.0000(10) | 2.9904(11) |
| Ln(3)−Se(1) | 3.1705(11) | 3.1507(13) | 3.1352(13) |
| Ln(3)−Se(6) | 3.2955(12) | 3.2642(14) | 3.2579(15) |
| Cr(1)−Se(4) × 2 | 2.5426(10) | 2.5526(11) | 2.5376(12) |
| Cr(1)−Se(6) × 4 | 2.6009(7) | 2.5965(8) | 2.5759(8) |
| Cr(2)−Se(2) × 2 | 2.4728(9) | 2.4713(11) | 2.4674(12) |
| Cr(2)−Se(5) × 4 | 2.6132(7) | 2.6246(8) | 2.6009(8) |

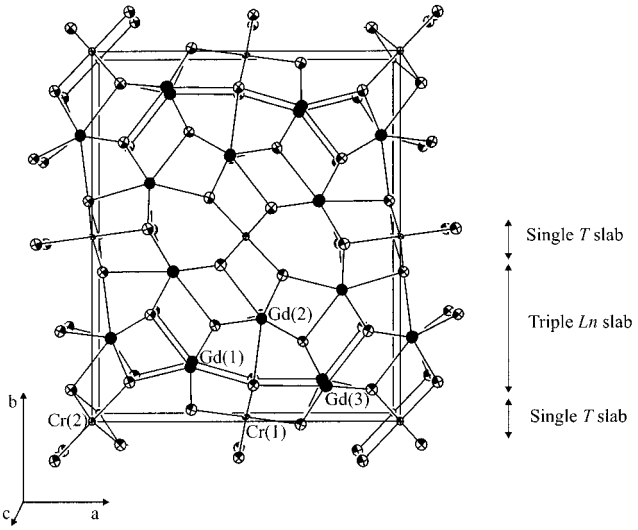


**Figure 1.** Perspective view of the structure of $Gd_3CrSe_6$ down *c*.

**Magnetic Studies** Magnetic measurements on polycrystalline powders were carried out with a SQUID magnetometer (MPMS5, Quantum Design). The samples, 38.7 mg of $Sm_3InSe_6$, 34.3 mg of $Sm_3CrSe_6$, 23.6 mg of $Gd_3CrSe_6$, and 31.5 mg of $Tb_3CrSe_6$, were loaded in gelatin capsules. Zero-field-cooled (ZFC) data were processed for $Sm_3InSe_6$ and $Ln_3CrSe_6$ (Ln = Sm, Tb) with 200 and 100 G applied field, respectively, in the temperature range 5−300 K, whereas for $Gd_3CrSe_6$ ZFC and field-cooled (FC) data were processed with 100 G applied field. Magnetization versus magnetic field measurements up to 5 T were also collected at 5 K for $Gd_3CrSe_6$. All data were corrected for electron core diamagnetism.[15]

## Results

**Crystal Structure Description.** The isostructural compounds $Ln_3TSe_6$ (Ln = Sm, Gd; T = In, Cr) and $Tb_3CrSe_6$ adopt the $U_3ScS_6$ structure type.[11] A projection of the three-dimensional structure of $Gd_3CrS_6$ along the *c* axis is displayed in Figure 1. There are three crystallographically independent Ln atoms in the cell. Atom Ln(1) is surrounded by seven Se atoms in a

(14) Yvon, K.; Jeitschko, W.; Parthé, E. *J. Appl. Crystallogr.* **1977**, *10*, 73−74.

(15) Mulay, L. N., Boudreaux, E. A., Eds. *Theory and Applications of Molecular Diamagnetism*; Wiley-Interscience: New York, 1976.

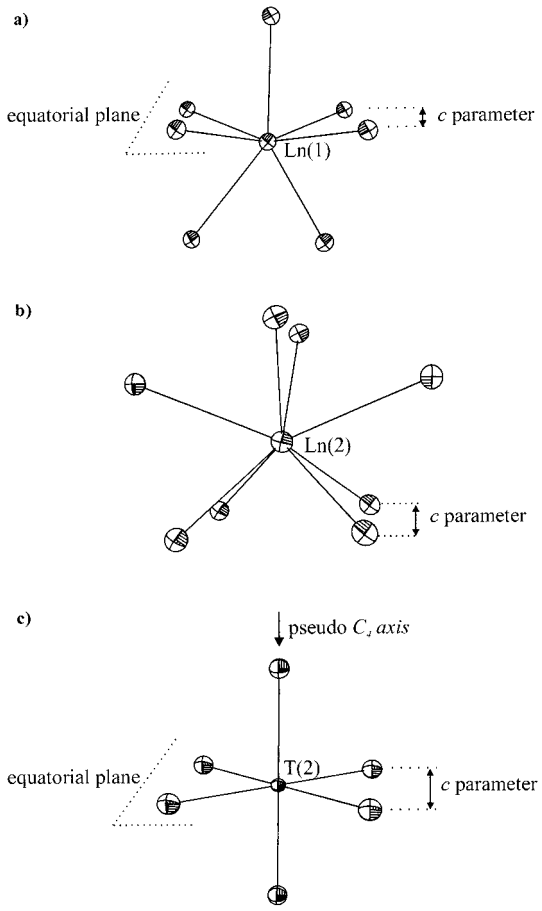


**Figure 2.** View of the environment of (a) Ln(1), (b) Ln(2), and (c) T(2) found in $Ln_3TSe_6$.

pseudo-octahedral arrangement with four Se atoms in the equatorial plane and three other Se atoms in a perpendicular plane; this arrangement is usually described as a 7-octahedron with one apex split into two positions (Figure 2a). Atoms Ln(2) and Ln(3) are surrounded by eight Se atoms in nominally a bicapped trigonal prismatic arrangement, the triangular faces being perpendicular to *c* (Figure 2b). However, for atom Ln(3) (Tables 2 and 3) the two Se atoms capping the rectangular faces of the trigonal prism centered by a cation are at least 0.1 Å longer than the sums of ionic radii[16] and have comparable interactions in the structure. This arrangement has been observed in rare-earth sesquichalogenides with the $U_2S_3$ structure type and is usually described as a "plus one" coordination number.[17] The In and Cr atoms are surrounded by six Se atoms in a slightly distorted octahedral arrangement formed by four equidistant Se atoms in an equatorial plane that is capped by two axial Se atoms along the pseudo 4-fold symmetry axis (Figure 2c). The $T(1)Se_6$ octahedra are almost regular, whereas $T(2)Se_6$ octahedra show longer T(2)−Se distances in the equatorial plane than in the axial direction. This can be rationalized in that the equatorial edges of $T(2)Se_6$ octahedra have to fit the *c* lattice constants, which are mainly determined by the heights of the trigonal prisms centered by the rare-earth cations (see Tables 2 and 3).

Since the *c* lattice constant corresponds to the height of a trigonal prism, the crystal structure can be described according to the orientation and linkage of the basic motif in the *ab* plane. Figure 3 displays a projection onto this plane of the packing

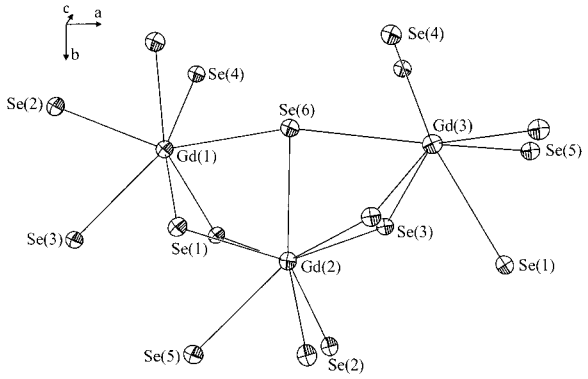


**Figure 3.** Projection view along *c* axis of the packing of rare-earth polyhedra.

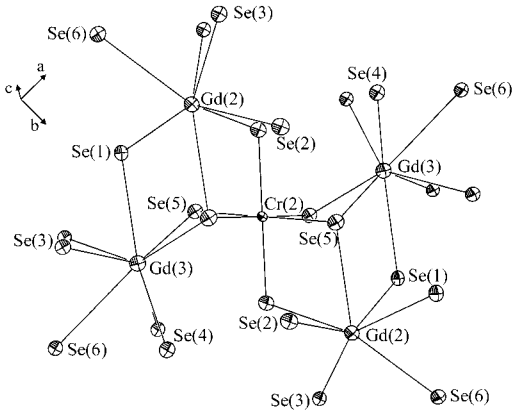


**Figure 4.** Projection along *c* axis of the packing around Cr(2) in $Gd_3CrSe_6$.

among polyhedra centered by the three independent rare-earth cations per unit cell. Each polyhedron shares two common edges in the *c* direction and a single Se atom (Se(6)), forming either the cap of a rectangular face for trigonal prismatic geometry or one apex for 7-octahedron geometry. This packing extends in the *a* direction to form a triple slab of rare-earth-centered polyhedra. In the *b* direction, rare-earth slabs are separated by a single transition element slab. The packing between three close layers is displayed in Figure 4. Octahedra centered by T(2) cations share a common edge in the *c* direction and a single Se atom with rare-earth trigonal prisms from each slab. The packing around the T(1) octahedra is slightly different in that they share along *c* the Se(6) atom, which is common to the three unique rare-earth polyhedra (see Figure 3).

In the present compounds, the Se ions adopt high coordination numbers; Se(1), Se(3), Se(4), Se(5), and Se(6) are surrounded by five cations in an irregular pyramidal geometry, whereas Se(2) is surrounded by four cations in a distorted tetrahedral geometry.

**Magnetic Properties.** The temperature dependence of the inverse magnetic susceptibility ($\chi^{-1}$) is displayed in Figure 5 for $Sm_3InSe_6$. The magnetic susceptibility does not follow a Curie−Weiss law. The curved shape of the plot is similar to that observed for $Sm_2Se_3$ (defect $Th_3P_4$ structure type[18]) and is characteristic of the van Vleck paramagnetic ion $Sm^{3+}$, for which a mixture of several energy levels occurs at high temperature, rendering the effective magnetic moment temperature-dependent.[19] Nevertheless, the experimental effective magnetic moment ($\mu eff_{exp}$) can be determined approximately

(16) Shannon, R. D. *Acta Crystallogr., Sect. A: Cryst. Phys., Diffr., Theor. Gen. Crystallogr.* **1976**, *32*, 751−767.
(17) Schleid, T. *Z. Anorg. Allg. Chem.* **1990**, *590*, 111−119.
(18) Grundmeier, T.; Heinze, T.; Urland, W. *J. Alloys Compd.* **1997**, *246*, 18−20.

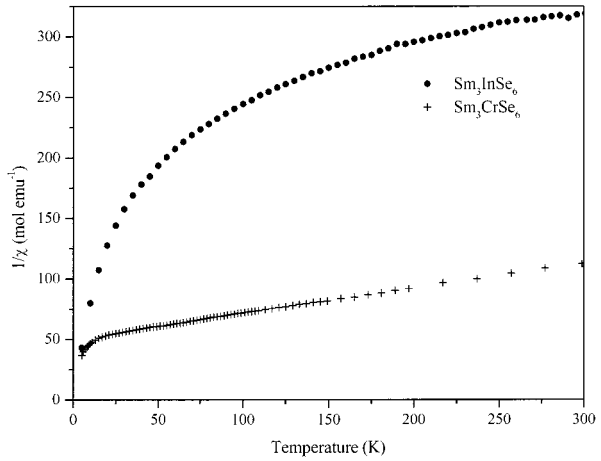


**Figure 5.** $\chi^{-1}$ vs $T$ for $Sm_3TSe_6$ (T = In, Cr).

from the relation $\mu eff_{exp} = [(3k_BT/N)\chi_m]^{1/2}\ \mu_B$, where $k_B$ is Boltzmann's constant, $T$ is the temperature in K, $N$ is Avogadro's number, and $\chi_m$ is the molar susceptibility in emu $mol^{-1}$. The resultant value of 1.58(2) $\mu_B$ at $T = 300$ K for the experimental effective moment per $Sm^{3+}$ may be compared with the values $\mu eff_{calc} = 1.55$ and 1.65 $\mu_B$ calculated with the van Vleck formula[19] for the screening numbers $\sigma = 33$ and 34, respectively. No dramatic change in the susceptibility occurs; $Sm_3InSe_6$ is thus paramagnetic in the temperature range 5−300 K.

The magnetic properties of $Sm_3CrSe_6$ (Figure 5) are dominated by the Sm cations, and consequently the magnetic susceptibility of $Sm_3CrSe_6$ does not obey the Curie−Weiss law $\chi = C/(T - \theta_p)$ despite a quasi-linear portion of the curve between 40 and 300 K. Hence, a Weiss constant cannot be extrapolated. Nevertheless, given that $Sm_3InSe_6$ and $Sm_3CrSe_6$ are isostructural and that the Sm−Se and Sm−Sm distances are in the same range for both compounds, we have taken the magnetic contribution of $Sm^{3+}$ determined at $T = 300$ K in $Sm_3InSe_6$ to be that in $Sm_3CrSe_6$ and hence have evaluated the magnetic contribution of the $Cr^{3+}$ cation at 300 K. The experimental effective moment calculated per $Cr^{3+}$ is 3.72(5) $\mu_B$, in good agreement with the theoretical spin-only effective moment of 3.87 $\mu_B$ per $Cr^{3+}$ calculated from the equation $\mu eff_{calc} = g[S(S + 1)]^{1/2}\ \mu_B$, where $g$ is the gyromagnetic ratio and $S$ is the sum of the spin quantum numbers of the individual unpaired electrons.[20]

Even though the magnetic susceptibility of neither Sm compound follows the Curie−Weiss law, the above results are consistent with the assignment of oxidation states Sm(III) and Cr(III), as already suggested by charge balance.

The magnetic susceptibility of $Gd_3CrSe_6$ (Figure 6) goes through a maximum around $T = 10(1)$ K and then drops sharply as the temperature increases, indicative of antiferromagnetic ordering. Since no magnetic ordering is observed in $Sm_3CrSe_6$ or $Tb_3CrSe_6$ (see below), this ordering in $Gd_3CrSe_6$ probably involves the $Gd^{3+}$ centers. The slight deviation observed on the ZFC−FC measurements suggests a small canting of the spins. The plot of magnetization versus magnetic field at 5 K (inset) exhibits a change in slope at low magnetic field, which may be attributed to a spin reorientation, in agreement with the expectation of a predominantly antiferromagnetic arrangement of the spins. No magnetic saturation was observed up to 5 T.

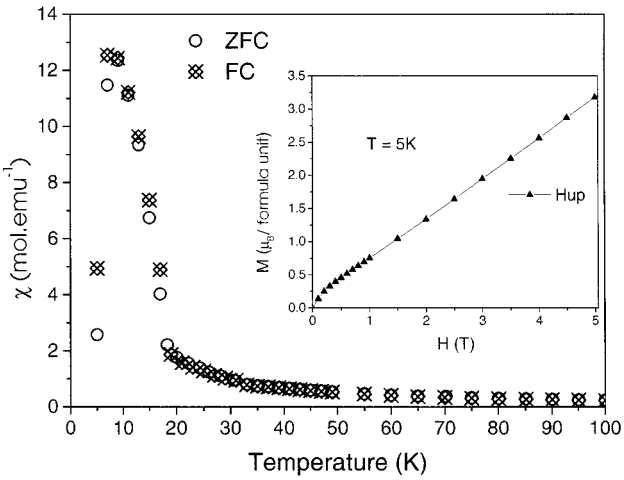


**Figure 6.** ZFC-FC measurements of $\chi$ vs $T$ for $Gd_3CrSe_6$. Inset shows magnetization vs magnetic field for $Gd_3CrSe_6$ at $T = 5$ K.

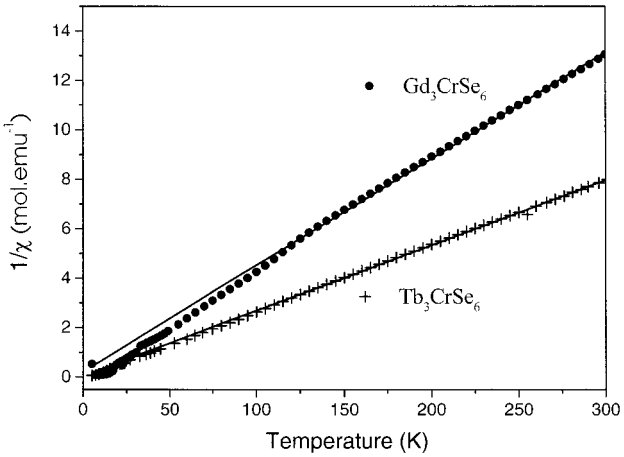


**Figure 7.** $\chi^{-1}$ vs $T$ for $Ln_3CrSe_6$ (Ln = Gd, Tb). The solid lines are the least-squares fits to the Curie−Weiss relation.

The upward and downward curves match each other almost perfectly. At zero applied field the small magnetic remanence observed is within the errors of measurement and hence cannot be used to confirm a canted antiferromagnetic structure below $T_N = 10(1)$ K. In the paramagnetic domain (Figure 7), the susceptibility of $Gd_3CrSe_6$ follows the Curie−Weiss law. Least-squares fitting of these data in the temperature range 100−300 K leads to the experimental values $\theta_p = -5(1)$ K and $C = 23.2(2)$ emu K $mol^{-1}$, for an effective moment $\mu eff_{exp} = 13.6(3)$ $\mu_B$ compared with the value $\mu eff_{calc} = 14.3\ \mu_B$, calculated from the Curie constants for $Gd^{3+}$ and $Cr^{3+}$ of 7.88 and 1.87 emu K $mol^{-1}$, respectively.[21] We do not know why there is a deviation from the Curie−Weiss law below 120 K.

Magnetic data for $Tb_3CrSe_6$ are displayed in Figure 7. This compound is paramagnetic down to 5 K. Least-squares fitting of these data in the temperature range 100−300 K to the Curie−Weiss law gives the experimental values $\theta_p = -2.0(9)$ K and $C = 37.9(2)$ emu K $mol^{-1}$, leading to $\mu eff_{exp} = 17.4(3)\ \mu_B$ to be compared with $\mu eff_{calc} = 17.3\ \mu_B$. Below 80 K magnetic data for $Tb_3CrSe_6$ show a small deviation from the Curie−Weiss law.

## Discussion

In the ternary systems Ln/In/Q, in addition to the present $Sm_3InSe_6$ and $Gd_3InSe_6$ compounds, there are eight compounds

(19) Van Vleck, J. H. *The Theory of Electric and Magnetic Susceptibilities*; Oxford University Press: London, 1932.
(20) Cotton, F. A.; Wilkinson, G. *Advanced Inorganic Chemistry*, 5th ed.; John Wiley & Sons: New York, 1988.
(21) Kittel, C. *Introduction to Solid State Physics*, 6th ed.; Wiley: New York, 1986.

known with the general formula $Ln_3InQ_6$. $Ln_3InS_6$ (Ln = Sm, Gd, Tb)[22] and $Pr_3InSe_6$[23] crystallize in the $U_3ScS_6$ structure type, although this was not previously recognized because of a different choice of origins. $Ln_3InS_6$ (Ln = La, Ce, Pr, Nd) crystallize in the $La_3InS_6$ structure type,[24] which differs from the $U_3ScS_6$ structure type because one In cation is tetrahedrally coordinated.

The present compounds $Ln_3CrSe_6$ (Ln = Sm, Gd, Tb) constitute a new family in Ln/Cr/Q systems. Several phases are known with different compositions and structures. These are for $Cr^{2+}$: $Ln_2CrS_4$ (Ln = Y and Dy−Yb),[25,26] $Ln_4CrQ_7$ (Ln = Y and Ho−Tm, Q = S; Ln = Dy, Q = Se),[27,28] and $Er_6Cr_2S_{11}$.[29] For $Cr^{3+}$ they are $LnCrQ_3$ (Ln = La−Sm, Q = S; Ln = La−Nd, Q = Se),[30,31] $LnCr_3S_6$ (Ln = Y, Gd, and Dy−Er),[32] $Gd_{2/3}Cr_2S_4$,[33] $Sm_{2/3}Cr_2S_4$,[34] and $La_{15.9}Cr_{5.4}S_{32}$.[35]

As we noted, the $U_3ScS_6$ structure type consists of edge sharing along the short *c* axis of bicapped trigonal prisms or 7-octahedra centered by $Ln^{3+}$ with octahedra centered by $T^{3+}$. What combinations of Ln = rare earth and T = trivalent 3d element do we expect to lead to this structure type? Trivalent 3d cations that generally exhibit octahedral coordination include $Ti^{3+}$, $V^{3+}$, $Cr^{3+}$, $Mn^{3+}$, and $Fe^{3+}$. Table 4, derived from examination of the crystal structures of the binary and ternary rare-earth chalcogenides,[5] summarizes the most common coordination environments around rare-earth cations. The Roman numeral in brackets is the coordination number and the subscripts are p = prism, which can be tri-, bi-, or monocapped, and o = octahedron or 7-octahedron.[36] Given the regions depicted in Table 4, some conjectures can be made concerning the compositions of $Ln_3TSe_6$ compounds that will adopt the $U_3ScS_6$ structure type. First, as the heavy lanthanides can also adopt coordination number 6, the ratio of ionic radii, $r(Ln^{3+})/r(T^{3+})$, must be large enough to avoid disorder. Hence, $Ln^{3+}$ from La to Ho, which exhibit coordination numbers 7 or 8, should be favored. But second, because the cationic radii of $Ln^{3+}$ and $T^{3+}$ govern the sizes of the polyhedra that are edge-shared along *c*, $r(Ln^{3+})/r(T^{3+})$ must be near unity in order for close packing to occur. Given the apparent inconsistent requirements for $r(Ln^{3+})/r(T^{3+})$, it may be that the range of $Ln_3TSe_6$ structures that will adopt the $U_3ScS_6$ structure type is rather narrow. Nevertheless, these conjectures serve as a guide in our search for additional members of the series.

**Table 4.** Most Common Environment for $Ln^{3+}$ Cations

| | La | Ce | Pr | Nd | Sm | Gd | Tb | Dy | Y | Ho | Er | Tm | Yb | Lu | Sc |
|---|---|---|---|---|---|---|---|---|---|---|---|---|---|---|---|
| $[IX_p]$ | ← | | | ···→ | | | | | | | | | | | |
| $[VIII_p][VII_o]$ | ←··· | | | | | | | | | | ···→ | | | | |
| $[VII_p][VI_o]$ | | | | | | | | ← | | | | ···→ | | | |
| $[VI_o]$ | | | | | | | | | | | | | ←··· | | → |

**Acknowledgment.** This research was supported by the U.S. National Science Foundation under Grant DM 97-09351. Use was made of the Central Facilities supported by the MRSEC program of the National Science Foundation (DMR96-32472) at the Materials Research Center of Northwestern University.

**Supporting Information Available:** X-ray crystallographic files in CIF format for the structure determinations of $Ln_3TSe_6$ (Ln = Sm, Gd; T = In, Cr) and $Tb_3CrSe_6$. This material is available free of charge via the Internet at http://pubs.acs.org.

IC9914802

(22) Messain, D.; Carré, D.; Laruelle, P. *Acta Crystallogr., Sect. B: Struct. Crystallogr. Cryst. Chem.* **1977**, *33*, 2540−2542.
(23) Aleandri, L. E.; Ibers, J. A. *J. Solid State Chem.* **1989**, *79*, 107−111.
(24) Carré, D.; Guittard, M.; Adolphe, C. *Acta Crystallogr., Sect. B: Struct. Crystallogr. Cryst. Chem.* **1978**, *34*, 3499−3501.
(25) Tomas, A.; Guittard, M.; Chevalier, R.; Flahaut, J. *C. R. Seances Acad. Sci., Ser. C* **1976**, *282*, 587−589.
(26) Tomas, A.; Chevalier, R.; Laruelle, P.; Bachet, B. *Acta Crystallogr., Sect. B: Struct. Crystallogr. Cryst. Chem.* **1976**, *32*, 3287−3289.
(27) Adolphe, C.; Laruelle, P. *Bull. Soc. Fr. Mineral. Cristallogr.* **1968**, *91*, 219−232.
(28) Souleau, C.; Guittard, M.; Wintenberger, M. *Bull. Soc. Chim. Fr.* **1966**, 1644−1645.
(29) Tomas, A.; Rigoult, J.; Guittard, M.; Pierre, L. *Acta Crystallogr., Sect. B: Struct. Crystallogr. Cryst. Chem.* **1980**, *36*, 1987−1989.
(30) Kikkawa, S.; Fujii, Y.; Miyamoto, Y.; Meerschaut, A.; Lafond, A.; Rouxel, J. *Mater. Res. Bull.* **1999**, *34*, 279−288.
(31) Huy-Dung, N.; Etienne, J.; Laruelle, P. *Bull. Soc. Chim. Fr.* **1971**, 2433−2437.
(32) Takahashi, T.; Ametani, K.; Yamada, O. *J. Cryst. Growth* **1974**, *24/25*, 151−153.
(33) Meerschaut, A.; Lafond, A.; Hoistad, L. M.; Rouxel, J. *J. Solid State Chem.* **1994**, *111*, 276−282.
(34) Lafond, A.; Cario, L.; van der Lee, A.; Meerschaut, A. *J. Solid State Chem.* **1996**, *127*, 295−301.
(35) Litteer, J. B.; Sirchio, S. A.; Fettinger, J. C.; Smolyaninova, V.; Eichorn, B. W.; Greene, R. L. *Chem. Mater.* **1999**, *11*, 1179−1182.
(36) Carré, D.; Flahaut, J.; Khodadad, P.; Laruelle, P.; Rodier, N.; Tien, V. *J. Solid State Chem.* **1973**, *7*, 321−336.